AIAA JOURNAL
Vol. 33, No. 9, September 1995

Experimental Testing of Diffusion Models in a Manipulated Turbulent Boundary Layer

J. Lemay*
Université Laval, Québec G1K 7P4, Canada
and
J. P. Bonnet† and J. Delville‡
Centre d'Études Aérodynamiques et Thermiques, Poitiers, France

An experimental investigation of the performances of one-point closure turbulent diffusion models is performed in an externally manipulated turbulent boundary layer. Detailed hot wire anemometry measurements are performed on a refined two-dimensional grid, allowing the terms of the transport equations of the turbulent stresses to be calculated. The turbulent diffusion terms as well as the convection, production, and viscous diffusion terms are then directly estimated. The dissipation terms of each Reynolds tensor component are estimated by use of local isotropy hypothesis ($\epsilon_{ij} = 2/3\epsilon\delta_{ij}$), ϵ being obtained by balancing the turbulent kinetic energy budget. The pressure-strain terms are then obtained by balancing the $\overline{u_i'u_j'}$ equations. The results are presented for a streamwise position located near the manipulator trailing edge ($x = 2\delta_0$). All of the measurements are performed at relatively large distances from the wall ($y^+ > 120$), allowing the minimization of the spatial integration effects of the probes. The balances show the modifications imposed to the classical turbulent boundary-layer equilibria. Knowledge of the different terms allows several experimental applications of the conventional turbulent diffusion models to be made. One-equation, k–ϵ, algebraic stress, and second-order principal hypothesis or closure models are tested. It is shown that conventional models, developed for equilibrium flows perform quite well in this configuration. Because of imbalance between terms, however, one-equation and k–ϵ models cannot be successful in predicting this flow; the algebraic stress model can be used, but only if starting far enough from the manipulator. Higher order closures should be correct, as confirmed by other authors' calculations.

Nomenclature

C_{ij} = convection term of Eq. (2)
D_{ij} = viscous diffusion term of Eq. (2)
G = turbulent diffusion function, one-equation model
H = shape factor
h = manipulator height
k = turbulent kinetic energy ($\overline{u_i'u_i'}/2$)
L = dissipation length function, one-equation model
l = manipulator chord length
P_{ij} = production term of Eq. (2)
p' = fluctuating pressure
Re_l = Reynolds number based on l
Re_θ = Reynolds number based on θ
T_{ij} = turbulent diffusion term of Eq. (2)
t = manipulator thickness
U_e = freestream velocity
$\overline{U_i}$ = i component of mean velocity
$\overline{u_i'u_j'}$ = ij component of the Reynolds stress tensor
x, x_1 = streamwise axis, x is 0 at the manipulator trailing edge
y, x_2 = transverse axis, y is 0 at the wall
z, x_3 = spanwise axis
$\Delta_{()}$ = relative uncertainty in a given measurement ()
δ = boundary-layer thickness
δ_{ik} = Kronecker symbol, 1 for $i = k$ and 0 otherwise
δ_0 = boundary-layer thickness at the manipulator trailing edge
ϵ = dissipation rate of turbulent kinetic energy
ϵ_{ij} = dissipation term of Eq. (2)
θ = momentum thickness
ν = fluid kinematic viscosity
ξ = normalized downstream distance x/δ_0
Π_{ij} = pressure-transport term of Eq. (2)
ρ = fluid density
Φ_{ij} = pressure-strain term of Eq. (2)
$\overline{()}$ = mean value
$()'$ = fluctuating value

Presented as Paper 94-2348 at the AIAA 25th Fluid Dynamics Conference, Colorado Springs, CO, June 20–23, 1994; received July 21, 1994; revision received Feb. 10, 1995; accepted for publication Feb. 15, 1995.

*Professor, Département de génie mécanique. Member AIAA.
†Research Director, Laboratoire d'Études Aérodynamiques, URA Centre National de la Recherche Scientifique 191.
‡Research Engineer, Laboratoire d'Études Aérodynamiques, URA Centre National de la Recherche Scientifique 191.

Introduction

DIFFERENT techniques aim at reducing turbulent drag. Among these techniques, the use of external manipulators, often called LEBUs (large-eddy breakup devices), has been extensively studied over the past 10 years. This passive technique consists of introducing a thin device (flat ribbon, airfoil, etc.), parallel to the wall somewhere in the external part of a turbulent boundary layer. Different device configurations (single, tandem, stacked, etc.) have been studied, both experimentally and computationally. Several article reviews are devoted to this subject; see, for example, Bushnell,[1] Coustols and Cousteix,[2] Savill et al.,[3] or Anders.[4]

It is now well recognized that external manipulators do not achieve net drag reduction in turbulent flat plate boundary layers (see, for example, the discussion reported by Choi[5]). In the present paper, we do not consider this flow from the drag reduction viewpoint. Rather, we consider the fact that it is interesting to make use of this out-of-equilibrium flow to provide experimental data which allows for testing or validating turbulence models or hypotheses. The purpose of this study is to present refined measurements of a large number of turbulent, one-point, statistical quantities or moments, in order to 1) to evaluate the principal terms of the balance equations for the Reynolds tensor components and 2) to be able to directly apply closure models on the experimental values. For example, the model expressing the third-order moments in terms of second-order ones can be used to "predict" the turbulent diffusion of the $\overline{u_i'u_j'}$ equations; one can then compare this prediction to the value of the turbulent diffusion evaluated from the measurement

of the third-order moments. A similar strategy has been previously employed by Cormack et al.,[6] using measurement profiles reported in the literature.

For the flow under study, as far as the transport equation of the turbulent kinetic energy k is concerned, it has been shown by Tenaud et al.[7] that the measurements are in good agreement with the computation (using a three-equation closure). In this previous article, it is pointed out that the experimental estimation of the k budget reported by Lemay[8] agrees well with the calculation results obtained by Tenaud et al.[9] and Tenaud.[10] Good agreement is found for the diffusion as well as for the dissipation terms (the experimental estimation of ϵ is equal to the remainder term of the k budget). These results give some confidence in the experimental procedure used in the present study.

The paper is organized as follows. The next section deals with the experimental apparatus and measurement procedure. In the third section, we present and discuss the balance of the transport equations of the components of the Reynolds tensor. The last section is devoted to the application of the turbulence models to the experimental data and to the comparisons between predicted and measured values. The diffusion parameter of a one-equation model, the diffusion term of the k–ϵ model, the algebraic stress model (ASM) hypothesis, and finally the diffusion terms of the full Reynolds stress model (RSM) are tested.

Experimental Procedure

Facilities

The experiments were carried out in the CEAT Turbulence Laboratory closed-loop wind tunnel. This low-speed facility has a 2-m-long test section with a 300 × 300 mm cross section. The Cartesian coordinate system is defined as follows: the x axis is in the flow direction ($x = 0$ at the manipulator trailing edge), the y axis is in the crossflow direction ($y = 0$ at the wall), and the z axis is in the spanwise direction. At the location corresponding to $x = 0$, the natural (unmanipulated) boundary layer is characterized by the following parameters: boundary-layer thickness (at $\overline{U}/U_e = 0.995$) $\delta_0 = 23.5$ mm, momentum thickness $\theta = 2.3$ mm, shape factor $H = 1.35$, and Reynolds number based on θ, $Re_\theta = 4000$. The single flat ribbon manipulator has the following characteristics: length $l = 25$ mm $= 1.1\delta_0$, thickness $t = 0.1$ mm $= 0.004\delta_0$, height in the boundary layer $h = 10$ mm $= 0.43\delta_0$, and chord Reynolds number $Re_l = 36{,}000$. The notation $\xi = x/\delta_0$ is used as the normalized downstream distance. All of the details of the measurement apparatus can be found in Lemay et al.[11,12] All of the flow velocities are measured by the hot-wire anemometry technique.

Constant temperature anemometers (TSI 1750) are used with single- and cross-wire probes. The single, normal wire is a modified miniature probe (TSI 1260 T1.5) operating with tungsten wire 0.5 mm in length and 2.5 μm in diameter. The cross-wire probe (TSI 1248 T1.5) operates with tungsten wires 1.25 mm in length and 4 μm in diameter.

Uncertainty Analysis

The uncertainty in the estimate of the various quantities is analysed in terms of bias of the measurement technique, statistical convergence of each sample, and propagation of individual errors associated with each variable into the final results.

Bias of the Measurement Technique

The bias introduced when using the hot-wire anemometry technique is influenced by several parameters. Among the most relevant as regards the present experiment, one must consider the turbulence intensity, the directional sensitivity of the wires, the influence of temperature variation (temperature drift in the closed-loop wind tunnel), the sensitivity variation due to wire aging, and the spatial integration effect of the different probes.

Although no bias error can be rigorously quantified, one can minimize it by use of an appropriate calibration procedure. The hot-wire probes have been systematically calibrated against velocity, temperature, and flow angle before each run (a typical run duration corresponds to less than 2 h). This procedure prevents wire aging problems and minimizes the bias error.

To limit the spanwise spatial averaging of our single-wire probe, we have considered the observations made by Johansson and Alfredsson.[13] They have pointed out that a sensor length of $L^+ = 14$ or 32 has no significant effect on the measurement of $\sqrt{\overline{u'^2}}/u_\tau$ providing that $y^+ > 40$. Moreover, Ligrani and Bradshaw[14] have observed that the measurements of the turbulent intensity, the skewness factor, and the flatness factor of u' are nearly independent of sensor length for $L^+ < 25$ (if $L/d > 160$). For $L^+ = 34$, they observed a negligible spanwise spatial averaging of the single wire probe for $y^+ > 100$. We also refer to Lemay et al.[11] for a detailed discussion of the limitations linked to spatial integration of the present single-wire probe ($L^+ \simeq 30$) and the resulting frequency response of the system. Considering these observations and discussions, we have decided to limit the regions of measurement to, typically, 120 wall units away from the wall ($y/\delta > 0.1$).

For the cross-wire probes ($L^+ \simeq 60$), the recommendations made by Browne et al.[15] have been considered. Their criteria ($L/d > 140$, $L/\eta < 5$ and $\Delta z/\eta < 3$) have also guided the restrictions imposed in the present investigation (closest measurement station $\xi = 2$ and closest distance from the wall $y^+ = 120$). These restrictions limit the bias due to the turbulence intensity and the spatial averaging. Additional comments concerning the spatial integration effects associated with the present cross-wire probes can be found in Lemay et al.[11]

These probes allow us to estimate the different moments involved in the equations considered in this investigation: $\overline{U}$ and $\overline{V}$; $\overline{u'^2}$, $\overline{v'^2}$, $\overline{w'^2}$, and $\overline{u'v'}$; and $\overline{u'^3}$, $\overline{u'^2v'}$, $\overline{u'v'^2}$, $\overline{v'^3}$, $\overline{u'w'^2}$, and $\overline{v'w'^2}$.

The analysis is performed at a measurement station located in the near wake of the manipulator ($\xi = 2$); in this region, one can observe important out of equilibrium behaviors. The measurements are performed following a grid which comprises longitudinal (x) and transverse (y) spacings. The spacings between the measurement points are reduced in the regions where strong spatial gradients are expected. The minimum separation in the y direction is 0.02δ and in the x direction is 0.3δ. The closest distance from the wall is 1.8 mm (0.08δ or $120y^+$). This procedure allows the proper estimation of the gradients involved, either in the transport equations of the Reynolds stresses, or in the turbulence models presently under investigation. The spatial derivatives are estimated using a conventional three-point central difference formulation (second-order precision).

In summary, the measurement grid and its location ($\xi = 2$) have been determined with respect to the integration effects of the different probes. The measurement points are always located far enough from either the wall or the manipulator trailing edge, thus limiting the integration problems which result from the spatial extent of the probes and the bias due to high turbulence intensity.

Statistical Convergence of Each Sample

For the single- and cross-wire measurements, the sampling rate is set to 50,000 samples/s and the sample sizes consist of 256,000 and 128,000 data points, respectively. For an integral time scale of 1 ms and a stationary Gaussian signal, this gives relative statistical convergence errors of less than 0.3% for $\overline{U}$, 2% for $\overline{u'^2}$ and 4% for $\overline{u'^4}$. For intermittent signals ($y/\delta > 0.7$), these errors become slightly larger.

Propagation of Errors

This part of the analysis is based on the method described by Kline and McClintock,[16] Coleman and Sleele,[17] and Steele and Coleman.[18] The propagation of individual errors into the results has been considered first when estimating the different moments ($\overline{U}_i$, $\overline{u_i'u_j'}$ and $\overline{u_i'u_j'u_k'}$). After this first step, the propagation of errors analysis then addressed the estimate of the terms appearing in the transport equations (e.g., T_{ij}, ϵ_{ij}, ...) or in the different models under investigation.

Based on these previous considerations, the uncertainties in the estimate of the moments are as follows: mean velocity ±0.5%, turbulence intensities ±3%, Reynolds shear stress ±5%, third-order moments ±5%($\overline{u'^3}$), ±7%($\overline{v'^3}$), and ±9% (cross components of the third-order moments).

The gradients of almost all of the different moments are used in the determination of the terms appearing in the transport equations and in the turbulence models. Based on a number of measurements (different probes), one can estimate the uncertainty in the resulting gradients. For example, the uncertainty in $\partial\overline{U}/\partial y$ is estimated to be less than $\pm 4\%$ and the uncertainty in T_k, which is the sum of several gradients of the third-order moments, is estimated to be approximately $\pm 15\%$.

Using the propagation of error analysis, one can then estimate Δ_0, the relative uncertainty in the terms of the transport equations. For the k equation, the following estimates are obtained: $\Delta_{C_k} = \pm 10\%$, $\Delta_{P_k} = \pm 7\%$, and $\Delta_{T_k} = \pm 15\%$. The dissipation term is obtained by balancing the k equation: $\epsilon = C_k - P_k - T_k$, since away from the wall the assumption of D_k and $\Pi_k \simeq 0$ is generally accepted. For example, the propagation of error analysis made in this case gives

$$\Delta_\epsilon = \sqrt{\left(\Delta_{C_k}\frac{C_k}{\epsilon}\right)^2 + \left(\Delta_{P_k}\frac{P_k}{\epsilon}\right)^2 + \left(\Delta_{T_k}\frac{T_k}{\epsilon}\right)^2} \qquad (1)$$

Using the k budget reported in Lemay et al.,[11] we obtain from Eq.(1) $\Delta_\epsilon = \pm 7\%$ near the wall ($y/\delta = 0.1$), $\Delta_\epsilon = \pm 11\%$ in the lower part of the manipulator wake ($y/\delta = 0.39$), and $\Delta_\epsilon = \pm 12\%$ in the upper part of the manipulator wake ($y/\delta = 0.46$). Near the wall ($y/\delta = 0.1$) the uncertainty in ϵ is low and approximately equal to Δ_{P_k} since at this location the production term is larger than the others ($P_k/\epsilon = -0.97$ compared with $C_k/\epsilon = -0.05$ and $T_k/\epsilon = 0.02$).

Finally, the uncertainty in the terms obtained using the turbulence models is rather difficult to estimate. The turbulent diffusion models under investigation are of the gradient diffusion type. The major part of the global uncertainty in these terms is that contribution due to the uncertainty in ϵ and that due to the gradients of the second-order moments. We estimate the uncertainty in the modeled diffusion terms to be of the order of ± 20–25%.

Reynolds Stress Budget

Transport Equations

The transport equations of the components of the Reynolds tensor $\overline{u_i'u_j'}$ are written with the following from (mean stationarity is assumed):

$$0 = \overbrace{-\overline{U}_k\frac{\partial\overline{u_i'u_j'}}{\partial x_k}}^{C_{ij}} \overbrace{-\left(\overline{u_i'u_k'}\frac{\partial\overline{U}_j}{\partial x_k} + \overline{u_j'u_k'}\frac{\partial\overline{U}_i}{\partial x_k}\right)}^{P_{ij}}$$
$$\overbrace{+\overline{\frac{p'}{\rho}\left(\frac{\partial u_i'}{\partial x_j} + \frac{\partial u_j'}{\partial x_i}\right)}}^{\Phi_{ij}} \overbrace{-\frac{\partial\overline{u_i'u_j'u_k'}}{\partial x_k}}^{T_{ij}} \overbrace{+\nu\frac{\partial^2\overline{u_i'u_j'}}{\partial x_k\partial x_k}}^{D_{ij}}$$
$$\underbrace{-\frac{\partial}{\partial x_k}\overline{\left(\frac{p'}{\rho}(u_i'\delta_{jk} + u_j'\delta_{ik})\right)}}_{\Pi_{ij}} \underbrace{-2\nu\overline{\frac{\partial u_i'}{\partial x_k}\frac{\partial u_j'}{\partial x_k}}}_{\epsilon_{ij}} \qquad (2)$$

As usual, the different terms appearing are classified from their physical meanings: C_{ij} is the convection, P_{ij} the production, T_{ij} the turbulent diffusion, D_{ij} the molecular or viscous diffusion, Π_{ij} the pressure-velocity effects or pressure-transport term, Φ_{ij} the pressure-strain interaction or redistribution term, and ϵ_{ij} the turbulent dissipation.

The dissipation term of each Reynolds tensor component is estimated by use of the local isotropy hypothesis ($\epsilon_{ij} = 2/3\epsilon\delta_{ij}$); ϵ is obtained by balancing the turbulent kinetic energy budget ($k = \overline{u_i'u_i'}/2$). This hypothesis is not in agreement with the direct numerical simulation (DNS) data reported, for example, by Mansour et al.[19] for the channel flow. For $y^+ > 50$ their data show that a model of the type $\epsilon_{ij} = (\overline{u_i'u_j'}/k)\,\epsilon$ should be more appropriate. Nevertheless, we have used the isotropic model, because first, it is still the standard assumption made in the RSM approach and, second, it does not influence the turbulent diffusion terms or models tested in the present paper. It only affects the estimation of the Φ_{ij} terms obtained by balancing the $\overline{u_i'u_j'}$ budget (2).

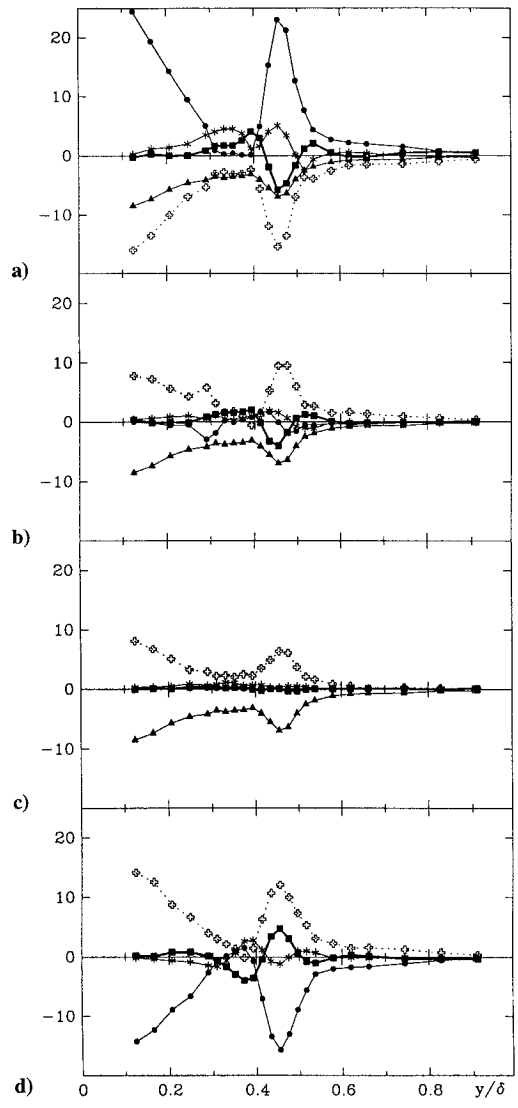

Fig. 1 Budget of the $\overline{u_i'u_j'}$ equations, normalization with $(U_e^3/\delta)\times 10^{-4}$: ⋆, convection; •, production; ■, diffusion; ▲, dissipation; and ✣, remainder; a) $\overline{u'^2}$, b) $\overline{v'^2}$, c) $\overline{w'^2}$, and d) $\overline{u'v'}$.

Results and Analysis of the $\overline{u_i'u_j'}$ Budgets

The balances of the transport equations of $\overline{u'^2}$, $\overline{v'^2}$, $\overline{w'^2}$, and $\overline{u'v'}$ are presented in Fig. 1. Analysis of this figure is performed by dividing the boundary layer in two parts following the transverse direction: region I corresponds to the lower part, located between the wall and the axis of the manipulator wake ($y/\delta < 0.43$) and part II is the upper part of the wake ($y/\delta > 0.43$). The wake of the manipulator does not develop symmetrically as does the usual unconfined turbulent wake. As it develops inside a wall-bounded $\overline{U}$ transverse gradient, the resulting evolution of $\partial\overline{U}/\partial y$ is quite different between regions I and II. Actually, at the downstream distance corresponding to $\xi = 2$, there is a large portion of region I ($0.25 \le y/\delta \le 0.4$) where $\partial\overline{U}/\partial y$ is very low (see the $\overline{U}$ profiles in Lemay[8]). A direct consequence of this fact is the noticeable difference between the P_{ij} terms (actually P_{11} and P_{12}) measured in regions I and II (Figs. 1a and 1d). In the lower part, close to the manipulator height, nearly all of the terms of the corresponding equations vanish, except the dissipation terms of the normal components.

The convection term is essentially important for $\overline{u'^2}$ and $\overline{u'v'}$ equations in this region. It should be noticed that, as in the natural case, the balance of the $\overline{w'^2}$ equation shows an equilibrium between pressure-strain and dissipation terms only. The modification of the diffusion

mechanisms imposed by the manipulation appears to be essentially a two-dimensional process lying in the xy plane.

In the outer region II, as previously guessed, an important increase of the production term is observed for $\overline{u'^2}$ (Fig. 1a) and $\overline{u'v'}$ (Fig. 1d). In the first case, the production excess is mainly balanced by the redistribution and, in a small part, by dissipation and diffusion. Indeed, this large redistribution rate is balanced by the excess of dissipation for the two other normal components (Figs. 1b and 1c), with the help of the diffusion for $\overline{v'^2}$. For the shear stress, Fig. 1d, the excess of production is balanced by pressure-strain and diffusion terms. Inside the manipulator wake, the diffusion of $\overline{u'v'}$ is a sink in region II and a source in the lower part, exactly as in the case of the turbulent kinetic energy budget, as previously noticed by Lemay et al.[11] This clearly illustrates the role of the diffusion in rearranging, essentially for $\overline{u'^2}$ and $\overline{u'v'}$, the imbalance due to the manipulation.

Testing of Turbulent Diffusion Models

As far as conventional, one-point numerical predictions of the manipulated flows are concerned, several levels of complexity are encountered. The one-equation approach, initially introduced by Bradshaw et al.,[20] has been used by Veuve,[21] k–ϵ closure was tested, for example, by Savill[22] and Tenaud et al.[9] Higher level models have also been applied to such flows, like algebraic stress model or Reynolds stress models (with five or three equations).[9,10,22,23] This list is not exhaustive but reflects the fact that external manipulation is an interesting test for closure models. Except for the work of Tenaud,[10] many calculations start downstream of the manipulator trailing edge and use the experimental data as boundary conditions. It is then somewhat difficult to compare calculations and experiments for the behavior of the models as we have done with the three-equation model in Tenaud et al.[7] We present now direct experimental tests of the turbulence models used by most of the aforementioned authors.

First, a remark has to be made. It concerns the usual assumption required by most of the lower level models, i.e., one-equation and k–ϵ. Indeed, in these cases, it is necessary to hypothesize the direct relationship between turbulent shear stress and kinetic energy. This relationship is far from being universal in the vicinity of the manipulator, as can be observed in Fig. 2.

It appears that the normal components are somewhat modified, but the distribution of the kinetic energy within its three components is not strongly affected by the manipulation. On the contrary, the variations of $\overline{u'v'}$ are much more important than those of k. One must mention, however, that such behavior rapidly vanishes downstream; we have observed (not presented here) that for $\xi \geq 7.5$ the relaxed, natural values are almost reached. This result clearly shows that the two first closure models cannot be successful if applied too closely to the manipulator, unless specific adaptations based on the experimental results are made as, for example, done by Veuve.[21] However, this observation does not mean that the closure models or other hypotheses involved in these models are not valid. One of the purposes of the present study then is to test the models by themselves. Subsequently, local experimental use of turbulence closure models can be done.

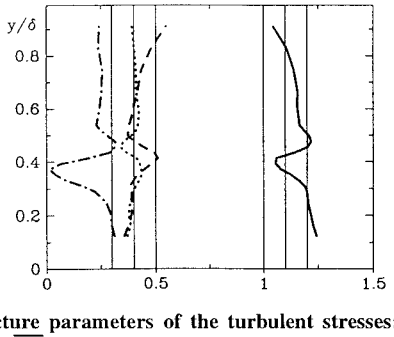

Fig. 2 Structure parameters of the turbulent stresses: $\overline{u'^2}/k$ (——), $\overline{v'^2}/k$ (– – – –), $\overline{w'^2}/k$ (· · · · · ·), and $-\overline{u'v'}/k$ (–·–).

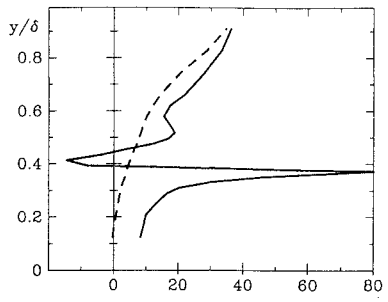

Fig. 3 Parameter G of the one-equation model, normalization with $(-\overline{u'v'})^{1/2}/U_e$; manipulated boundary layer (——), conventional value (- - - -) after Bradshaw et al.[20]

One-Equation Modeling

The one-equation closure model proposed by Bradshaw et al.[20] is based on a relationship between the turbulent shear stress and the turbulent kinetic energy (structure parameter $a_1 = -\overline{u'v'}/k$), associated with the transport equation of k. This model requires a specific function G for the turbulent diffusion and a specific length L for the dissipation.

G is defined as

$$G = \frac{\overline{u'^2v'} + \overline{v'^3} + \overline{v'w'^2} + \frac{1}{\rho}\overline{p'v'}}{-\overline{u'v'}(-\overline{u'v'}_{\max})^{\frac{1}{2}}} \tag{3}$$

L is defined as

$$L = \frac{(-\overline{u'v'})^{\frac{3}{2}}}{\epsilon} \tag{4}$$

As usual, the experimental estimation of G, defined by Eq. (3), is obtained by neglecting the term $\overline{p'v'}$.

The diffusion function G is plotted in Fig. 3. As expected, this function is strongly altered. It should be noticed that, if in the vicinity of the manipulator $\overline{u'v'}$ vanishes, this is not the case for k. Then the value of G becomes unrealistic. As already mentioned, the application of the one-equation model can only be valid if the calculations start far enough from the manipulator.

k–ϵ Modeling

Gradient-Diffusion Models

In turbulence modeling, the third-order moments are frequently estimated using a gradient-diffusion hypothesis. Following this idea, the simplest form used to model the turbulent transport of a quantity ϕ in the x_j direction is given by

$$T_\phi = -\frac{\partial \overline{u_i'\phi'}}{\partial x_j} = \frac{\partial}{\partial x_j}\left(C_\phi \frac{k}{\epsilon}\overline{u_j'u_l'}\frac{\partial \phi}{\partial x_l}\right) \tag{5}$$

Equation (5) applied to the turbulent kinetic energy ($\phi = k$) and to the Reynolds stress ($\phi = u_i'u_j'$), gives the popular model proposed by Daly and Harlow.[24] For the RSM applications, however, this model is not rotationally invariant, because the expression is altered under permutation of the indices i, j, and k. To avoid this problem, Hanjalic and Launder[25] have proposed an alternate model for the triple correlations:

$$-\overline{u_i'u_j'u_k'} = C_s\frac{k}{\epsilon}\left(\overline{u_i'u_l'}\frac{\partial \overline{u_j'u_k'}}{\partial x_l} + \overline{u_j'u_l'}\frac{\partial \overline{u_i'u_k'}}{\partial x_l} + \overline{u_k'u_l'}\frac{\partial \overline{u_i'u_j'}}{\partial x_l}\right) \tag{6}$$

This model is more complicated than those based on the simplest form of the gradient-diffusion hypothesis, but it does not sacrifice the principle of Galilean invariance. In the present investigation, the results (T_k and T_{ij}) obtained with Hanjalic–Launder model are very similar to those obtained with Daly–Harlow model. Thus, the results based on Eq. (6) are not presented.

Several authors have recently compared different components of the triple correlations with those estimated by the Hanjalic–Launder and Daly–Harlow models; see, for example, Cazalbou and Bradshaw[26] (DNS in channel flow and two-dimensional

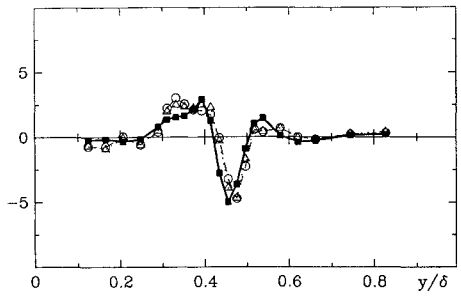

Fig. 4 Diffusion terms of the k equation, normalization with $(U_e^3/\delta) \times 10^{-4}$: ■, T_k from direct estimation; ○, T_k from Shir[30] model; and △, T_k from Daly and Harlow[24] model.

boundary-layer flow), Schwarz and Bradshaw[27] (measurement in three-dimensional boundary-layer flow), Skåre and Krogstad[28] (measurement in a two-dimensional boundary-layer flow in the presence of strong adverse pressure gradients), and Aronson and Löfdahl[29] (measurement in the plane wake of a cylinder). From these papers, for the two-dimensional flows, a general observation can be made: the measured triple correlation profiles and the profiles obtained from the models possess similar shapes although they are sometimes different in amplitude. This point is very important because, for the purpose of the turbulent diffusion modeling, the transverse gradient is rather more important than the actual value of the third-order moments. One must also note that most of the models use the time scale k/ϵ. The comparisons are then quite dependent on the reliability of the method used in estimating the dissipation rate of turbulent kinetic energy.

Results

The present measurements allow the estimation of the distribution of the second-order moments in an x–y grid; it is then possible to calculate their derivatives and, finally, the terms appearing in the closure models for the diffusion terms. Two models have been tested: the model proposed by Daly and Harlow[24] and its contracted form after Shir.[30]

The diffusion term of the k equation, modeled after Shir,[30] is

$$T_k = \frac{\partial}{\partial x_j}\left(\frac{C_\mu}{\sigma_k}\frac{k^2}{\epsilon}\frac{\partial k}{\partial x_j}\right) \tag{7}$$

The diffusion term of the k equation, modeled after Daly and Harlow,[24] is

$$T_k = \frac{\partial}{\partial x_j}\left(C_d\frac{k}{\epsilon}\overline{u_j'u_l'}\frac{\partial k}{\partial x_l}\right) \tag{8}$$

The values $C_\mu = 0.09, C_d = 0.22$, and $\sigma_k = 1.0$ have been adopted.

Figure 4 represents the experimental values of the diffusion terms, obtained by space derivatives of the directly measured third-order correlations. The application of the models, using the measured second-order correlations, leads to the open symbols plotted on the figure. The agreement between the three values is remarkable, despite the very intricate spatial distributions (already noted in the discussion for the equation budgets). The differences between the experimentally modeled terms and the directly measured ones are within the experimental uncertainties. This excellent agreement has been previously noticed by Tenaud et al.[7] when they compare three-equation model calculations (k–ϵ–$\overline{u'v'}$) with the present results. In this case, the diffusion terms coming from the calculations were the result of integration from upstream of the manipulator. In Fig. 4, on the contrary, the model is locally applied; however, since the three-equation model makes very good predictions of the turbulent profiles, the conclusions of Tenaud et al.[7] and the present ones are consistent. They indirectly validate the experimental estimation of the dissipation that appears explicitly in the scaling of the model.

Algebraic Stress Modeling

The ASM model avoids making use of a universal structure parameter of the Reynolds tensor or Boussinesq hypothesis. The closure is obtained by using a set of algebraic equations relating the different components of the Reynolds tensor. To derive an explicit form for $\overline{u_i'u_j'}$, a set of algebraic equations can be obtained if the following relationship is verified:

$$(C_{ij} - T_{ij}) = (C_k - T_k)\,\overline{u_i'u_j'}/k \tag{9}$$

This means that one assumes that the convective transport of $\overline{u_i'u_j'}$ occurs at the same rate as for k. Following the ASM approach, we choose in the present study to compare the experimental values of the term $(C_{ij} - T_{ij})$ with the values of the term $(C_k - T_k)\overline{u_i'u_j'}/k$. The terms $(C_{ij} - T_{ij})$ and $(C_k - T_k)$ represent the difference between convection and diffusion of $\overline{u_i'u_j'}$ and k, respectively.

Figure 5 presents the comparisons obtained for the four moments. The equivalence of the transport processes can be accepted with confidence mainly for $\overline{u'^2}$ but is somewhat in error for $\overline{v'^2}$ in region II and in region I for $\overline{w'^2}$. The inapplicability of the ASM hypothesis is more evident on the shear stress (Fig. 5d). Indeed, as Figs. 5a–5d together with Fig. 2 indicate, the convection practically balances the diffusion of k in region II (see, also, Lemay et al.[11]); that is not the case for $\overline{u'v'}$ (Fig. 5d or Fig. 1d). On the other hand, in region I, the quasivanishing value of $\overline{u'v'}$ in the lower part of the wake induces a very low value of the comparison term in the region where large imbalance exists in the convection/diffusion of $\overline{u'v'}$.

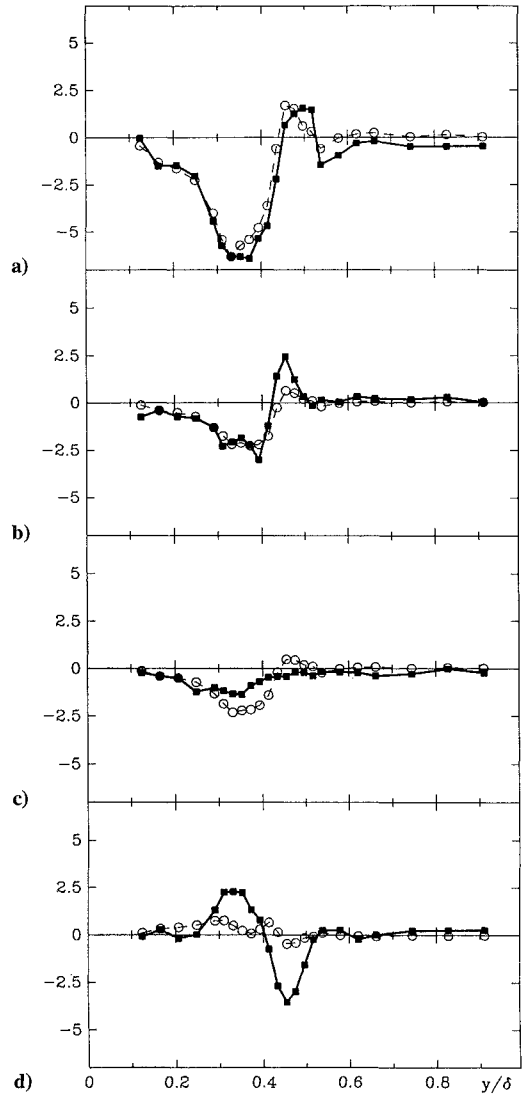

Fig. 5 Test of the algebraic stress model hypothesis, normalization with $(U_e^3/\delta) \times 10^{-4}$); ■, $C_{ij} - T_{ij}$; ○, $[C_k - T_k]\,\overline{u_i'u_j'}/k$; a) $\overline{u'^2}$ component, b) $\overline{v'^2}$, c) $\overline{w'^2}$, and d) $\overline{u'v'}$.

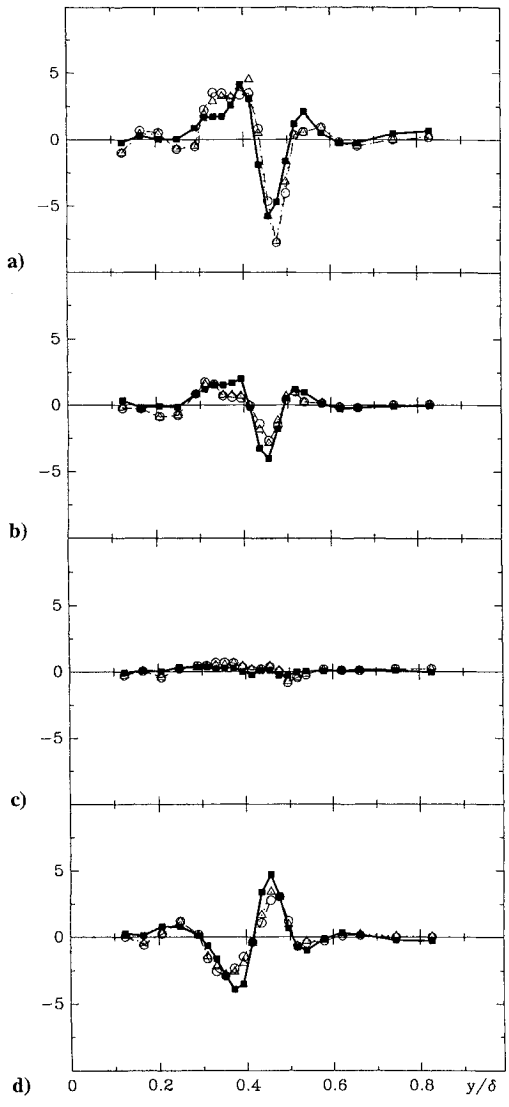

Fig. 6 Diffusion terms of the $\overline{u_i'u_j'}$ equations, normalization with $(U_e^3/\delta) \times 10^{-4}$: ■, T_{ij} from Eq. (2); ○, T_{ij} from Shir[30] model; and △, T_{ij} from Daly and Harlow[24] model; a) $\overline{u'^2}$ component, T_{11}; b) $\overline{v'^2}$, T_{22}; c) $\overline{w'^2}$, T_{33}; and d) $\overline{u'v'}$, T_{12}.

Full Reynolds Stress Modeling

The models tested and the technique for the comparison of experimental predictions and measurements are the same as those used for the test of the k equations (7) and (8).

The diffusion term of the $\overline{u_i'u_j'}$ equation, modeled after Shir,[30] is

$$T_{ij} = \frac{\partial}{\partial x_k}\left(\frac{C_\mu}{\sigma_k}\frac{k^2}{\epsilon}\frac{\partial \overline{u_i'u_j'}}{\partial x_k}\right) \tag{10}$$

The diffusion term of the $\overline{u_i'u_j'}$ equation, modeled after Daly and Harlow,[24] is

$$T_{ij} = \frac{\partial}{\partial x_k}\left(C_d\frac{k}{\epsilon}\overline{u_k'u_l'}\frac{\partial \overline{u_i'u_j'}}{\partial x_l}\right) \tag{11}$$

The results are reported in Fig. 6. As for T_k, the measured values of T_{11}, T_{22}, T_{33}, and T_{12} are in very good agreement with the experimental applications of the models. Both the Daly–Harlow and Shir models perform quite well in this flow and are well suited to describe the very different behaviors of, for example, $\overline{u'^2}$ and $\overline{w'^2}$. Unlike for $\overline{u'^2}$, the diffusion of $\overline{w'^2}$, as mentioned in the third section, is very low. The two models are well adapted to diffusion terms even in such an out-of-equilibrium flow.

This particular aspect can be further analyzed if one writes, for example, the explicit modeled form of T_k. Using the standard boundary-layer approximation ($\partial/\partial x \ll \partial/\partial y$) and with the corresponding value of each constant, this gives

$$T_k \simeq \frac{\partial}{\partial y}\left(0.09\frac{k^2}{\epsilon}\frac{\partial k}{\partial y}\right) \tag{12}$$

for the Shir model and

$$T_k \simeq \frac{\partial}{\partial y}\left(0.22\frac{k}{\epsilon}\overline{v'^2}\frac{\partial k}{\partial y}\right) \tag{13}$$

for the Daly–Harlow model.

For a natural boundary-layer case, a local equilibrium assumption can be made, and a standard value of $\overline{v'^2}/k \simeq 0.41$ can be used. This assumption applied to Eq. (13) gives

$$T_k \simeq \frac{\partial}{\partial y}\left(0.22\frac{k^2}{\epsilon}\frac{\overline{v'^2}}{k}\frac{\partial k}{\partial y}\right)$$

$$\simeq \frac{\partial}{\partial y}\left(0.09\frac{k^2}{\epsilon}\frac{\partial k}{\partial y}\right) \tag{14}$$

which is equivalent to Eq. (12), the Shir model. This analysis gives the same results for each of the T_{ij} terms.

For the manipulated case, it is noted from Fig. 2 that the ratio $\overline{v'^2}/k$ departs slightly from the standard value (> 0.41) only in the regions $0.37 < y/\delta < 0.46$ and $y/\delta > 0.7$. As expected, from Fig. 4 it can be seen that in these regions $|T_{k\text{D–H}}| > |T_{k\text{Shir}}|$, but the differences between the two models are quite small.

Finally, mention must be made that the agreement between the actual and modeled values of T_k and T_{ij} does not mean that the magnitude of the $\overline{u_i'u_j'u_k'}$ components are accurately modeled. This only means that the shape of the $\overline{u_i'u_j'u_k'}$ profiles are well reproduced. The models perform especially well when reproducing the transverse gradient of $\overline{u'^2v'}$, $\overline{v'^3}$, $\overline{v'w'^2}$, and $\overline{u'v'^2}$. Similar observations have been made by Schwarz and Bradshaw[27] in the two-dimensional region of their experiment (three-dimensional boundary-layer flow). They have shown that in a two-dimensional boundary layer the models are able to predict the general shape of the $\overline{u_i'u_j'u_k'}$ profiles.

Conclusion

The present detailed experiments have proven the ability of experimental approaches to perform validations of calculation hypotheses and closure models. The flow under consideration is, in some sense, enough out of equilibrium to provide a test case with a large amount of modifications when compared with the canonical case but is not too far from equilibrium to allow the use of conventional approaches. Most of the conclusions drawn from the calculations by several other authors have been directly checked by the present work, including limitations and possibilities of simple prediction methods, and the power of the high-level models. The analysis of the balance of transport equations of Reynolds stresses is a powerful tool for choosing the closure level. In addition, this study allows one to validate closure models by performing experimental closures. This can be a way to define or develop new closure models. In the present study, we have restricted the analysis to existing models with their conventional set of constants.

References

[1]Bushnell, D. M., "Turbulent Drag Reduction for External Flows," AGARD Rept., Vol. 193, 1985.

[2]Coustols, E., and Cousteix, J., "Réduction du frottement turbulent: modérateurs de turbulence," *La Recherche Aérospatiale*, No. 2, 1986, pp. 145–160 (in French).

[3]Savill, A. M., Truong, T. V., and Ryhming, I. L., "Turbulent Drag Reduction by Passive Means: a Review and Report on the First European Drag Reduction Meeting," *Journal of Theoretical and Applied Mechanics/Journal de Mécanique Théorique et Appliquée*, Vol. 7, 1988, pp. 353–378.

[4]Anders, J. B., "Outer-Layer Manipulators for Turbulent Drag Reduction," *Viscous Drag Reduction in Boundary Layers*, edited by D. M. Bushnel and J. N. Hefner, Vol. 123, Progress in Astronautics and Aeronautics, AIAA, Washington, DC, 1990, pp. 263–284.

[5]Choi, K. S., "Report on the 5th European Drag Reduction Working Meeting," *ERCOFTAC Bulletin* (European Research Community on Flow—Turbulence and Combustion), Vol. 8, March 1991, pp. 18–20.

[6]Cormack, D. E., Leal, L. G., and Seinfeld, J. H., "An Evaluation of Mean Reynolds Stress Turbulence Models: The Triple Velocity Correlation," *Journal of Fluids Engineering*, Vol. 100, March 1978, pp. 47–54.

[7]Tenaud, C., Lemay, J., Bonnet, J. P., and Delville, J.,"Balance of Turbulent Kinetic Energy Downstream a Single Flat Plate Manipulator: Comparisons Between Detailed Experiments and Modeling," *Turbulence Control by Passive Means*, edited by E. Coustols, Kluwer Academic, Norwell, MA, 1990, pp. 1–21.

[8]Lemay, J., "Étude expérimentale du comportement de la turbulence dans une couche limite incompressible en présence d'un manipulateur externe," Ph.D. Thesis, Département de génie mécanique, Univ. Laval, Québec, Canada, May 1989 (in French).

[9]Tenaud, C., Coustols, E., and Cousteix, J., "Modeling of Turbulent Boundary Layers Manipulated with Thin Outer Layer Devices," *Proceedings of the International Conference on Turbulent Drag Reduction by Passive Means*, Royal Aeronautical Society, London, 1987, pp. 114–168.

[10]Tenaud, C., "Simulation numérique de l'écoulement autour d'un manipulateur externe de couche limite," Ph.D. Thesis, École Nationale Supérieure de l'Aéronautique et de l'Espace, Toulouse, France, Sept. 1988 (in French).

[11]Lemay, J., Delville, J., and Bonnet, J. P., "Turbulent Kinetic Energy Balance in a LEBU Modified Turbulent Boundary Layer," *Experiments in Fluids*, Vol. 9, No. 6, 1990, pp. 301–308.

[12]Lemay, J., Savill, A. M., Bonnet, J. P., and Delville, J.,"Some Similarities Between Turbulent Boundary Layers Manipulated by Thin and Thick Flat Plate Manipulators," *Turbulent Shear Flows*, Vol. 6, edited by J. C. André, J. Cousteix, F. Durst, B. E. Launder, F. W. Schmidt, and J. H. Whitelaw, Springer–Verlag, Berlin, 1989, pp. 179–193.

[13]Johansson, A.V., and Alfredsson, P. H., "Effects of Imperfect Spatial Resolution on Measurements of Wall-Bounded Turbulent Shear Flows," *Journal of Fluid Mechanics*, Vol. 137, Dec. 1983, pp. 409–421.

[14]Ligrani, P. M., and Bradshaw, P., "Spatial Resolution and Measurement of Turbulence in the Viscous Sublayer Using Subminiature Hot-Wire Probes," *Experiments in Fluids*, Vol. 5, No. 6, 1987, pp. 407–417.

[15]Browne, L. W. B., Antonia, R. A., and Shah, D. A., "Selection of Wires and Wire Spacing for X-Wires," *Experiments in Fluids*, Vol. 6, No. 4, 1988, pp. 286–288.

[16]Kline, S. J., and McClintock, F. A., "Describing Uncertainties in Single-sample Experiments," *Mechanical Engineering*, Vol. 75, Jan. 1953, pp. 3–8.

[17]Coleman, H. W., and Steele, W. G., "Some Considerations in the Propagation of Bias and Precision Errors into an Experimental Result," *Experimental Uncertainty in Fluid Measurements*, edited by E. P. Rood, American Society of Mechanical Engineers, Fluids Engineering Div., Vol. 58, 1987, pp. 57–62.

[18]Steele, W. G., and Coleman, H. W., "Use of Uncertainty Analysis in the Planning and Design of an Experiment," *Experimental Uncertainty in Fluid Measurements*, edited by E. P. Rood, American Society of Mechanical Engineers, Fluids Engineering Div., Vol. 58,1987, pp. 63–67.

[19]Mansour, N. N., Kim, J., and Moin, P., "Reynolds-Stress and Dissipation-Rate Budgets in a Turbulent Channel Flow," *Journal of Fluid Mechanics*, Vol. 194, Sept. 1988, pp. 15–44.

[20]Bradshaw, P., Ferris, D. H., and Atwell, N. P., "Calculation of Boundary-Layer Development Using the Turbulent Energy Equation," *Journal of Fluid Mechanics*, Vol. 28, Pt. 3, April 1967, pp. 593–616.

[21]Veuve, M., Ph.D. Thesis, No. 768, Mechanical Engineering Dept., Swiss Federal Inst. of Technology, Lausanne, Switzerland, 1988.

[22]Savill, A. M., "Algebraic and Reynolds Stress Modeling of Manipulated Boundary Layers Including Effects of Free-Stream Turbulence," *Proceedings of the International Conference on Turbulent Drag Reduction by Passive Means*, Royal Aeronautical Society, London, 1987, pp. 89–143.

[23]Savill, A. M., "Turbulent Boundary Layer Manipulation and Modeling in Zero and Adverse Pressure Gradients," *Proceedings of the International Union of Theoretical and Applied Mechanics Turbulence Management and Relaminarization Symposium* (Bangalore, India), Springer–Verlag, Berlin, 1987, pp. 69–83.

[24]Daly, B. J., and Harlow, F. H., "Transport Equations in Turbulence," *Physics of Fluids*, Vol. 13, No. 11, 1970, pp. 2634–2649.

[25]Hanjalic, K., and Launder, B. E., "A Reynolds Stress Model of Turbulence and its Application to Thin Shear Flows," *Journal of Fluid Mechanics*, Vol. 52, Pt. 4, 1972, pp. 609–638.

[26]Cazalbou, J. B., and Bradshaw, P., "Turbulent Transport in Wall-Bounded Flows. Evaluation of Model Coefficients Using Direct Numerical Simulation," *Physics of Fluids A*, Vol. 5, No. 12, 1993, pp. 3233–3239.

[27]Schwarz, W. R., and Bradshaw, P., "Term-by-Term Tests of Stress-Transport Turbulence Models in a Three-Dimensional Boundary Layer," *Physics of Fluids A*, Vol. 6, No. 2, 1994, pp. 986–998.

[28]Skåre, P. E., and Krogstad, P. Å., "A Turbulent Equilibrium Boundary Layer Near Separation," *Journal of Fluid Mechanics*, Vol. 272, Aug. 1994, pp. 319–348.

[29]Aronson, D., and Löfdahl, L., "The Plane Wake of a Cylinder: Measurements and Inferences on Turbulence Modeling," *Physics of Fluids A*, Vol. 5, No. 6, 1993, pp. 1433–1437.

[30]Shir, C. C., "A Preliminary Numerical Study of Atmospheric Turbulent Flows in the Idealized Planetary Boundary Layer," *Journal of the Atmospheric Sciences*, Vol. 30, No. 7, 1973, pp. 1327–1339.